Cement and Concrete Research 100 (2017) 341–349

Contents lists available at ScienceDirect

Cement and Concrete Research

journal homepage: www.elsevier.com/locate/cemconres

Mechanical properties and microscale changes of geopolymer concrete and Portland cement concrete containing micro-encapsulated phase change materials

Shima Pilehvar[a,b], Vinh Duy Cao[a,c], Anna M. Szczotok[a,d], Luca Valentini[e], Davide Salvioni[f], Matteo Magistri[f], Ramón Pamies[b], Anna-Lena Kjøniksen[a,*]

[a] Faculty of Engineering, Østfold University College, P.O. Box 700, 1757 Halden, Norway
[b] Department of Material Engineering and Manufacturing, Technical University of Cartagena, Cartagena, Murcia, Spain
[c] Department of Mathematical Science and Technology, Norwegian University of Life Science, N-1432 Ås, Norway
[d] Department of Chemical Engineering, University of Castilla – La Mancha, 13004 Ciudad Real, Spain
[e] Department of Geosciences, University of Padua, 35131 Padua, Italy
[f] Mapei S.p.A. R & D Central Laboratory, Milan, Italy

ARTICLE INFO

Keywords:
Geopolymer concrete
Portland cement concrete
Micro-encapsulated phase change materials
Compressive strength
Microstructure

ABSTRACT

The effect of micro-encapsulated phase change materials (MPCM) in solid and liquid states on the mechanical properties and microstructure of geopolymer and Portland cement concretes is investigated. Geopolymer concrete (GPC) and Portland cement concrete (PCC) containing different amounts of MPCM were prepared and cured at both 20 °C and 40 °C. The results revealed that the compressive strength of both GPC and PCC decreases with the addition of MPCM. Whether the PCM is in solid (20 °C) or liquid (40 °C) state did not significantly affect the mechanical properties of GPC, while melting the PCM was found to reduce the strength of PCC. X-ray tomography imaging was utilized to examine the effect of MPCM on the porosity of the samples. SEM imaging reveals that air gaps are formed between the microcapsules and the surrounding concrete matrix.

1. Introduction

Phase change materials (PCM) have attracted the interest of the scientific community due to the possibilities of increasing of the thermal energy storage in buildings. Utilization of PCM will reduce the energy demand, and thereby contribute to a better environment. During the daytime, PCM absorbs excess heat by melting. The heat is released when the temperature decreases at night, causing the PCM to solidify [1]. Due to the high latent heat capacity of PCM, a considerable amount of heat energy can be stored during the phase change [1,2]. However, utilizing bulk quantities of PCMs is subject to problems. A low thermal conductivity causes bulk amounts of PCM to solidify only around the edges preventing a good heat transfer process [2,3]. These problems can be avoided by encapsulating the PCM into microcapsules. These microcapsules can then be incorporated into building materials, such as concrete, in order to create a smart material suitable for passive house construction. Incorporating micro-encapsulated PCM (MPCM) in structural materials significantly improves thermal energy storage. However, MPCM has been found to reduce the mechanical properties of building materials [4].

In recent years, the effect of PCMs and MPCMs on the mechanical properties of structural materials especially cementitious materials such as mortar and concrete has been studied at various curing conditions. Unfortunately, the presence of MPCM decreases the mechanical strength of concrete [5–9]. Several factors have been suggested to contribute to this strength reduction. When MPCMs replaces a certain percentage of sand, the mechanical strength decreases due to lower stiffness and strength of MPCM compared to sand [6]. In addition, rupture of the capsules during the mixing process and compression may cause leakage of PCM into the cementitious materials thereby reducing the strength [7]. PCM might induce voids and air bubbles, which also reduces the concrete strength [8]. In addition, weak bonds between the MPCM and the binder matrix can lead to interfacial gaps between MPCM and the concrete matrix [9].

Geopolymer is an attractive alternative to ordinary Portland cement. The negative environmental impact and high cost of Portland cement production can be significantly improved by replacing it with geopolymers [10,11]. Several studies have been conducted on the mechanical properties of geopolymer compositions [12–15] and a few studies have focused on cementitious materials with incorporated

* Corresponding author.
E-mail address: anna.l.kjoniksen@hiof.no (A.-L. Kjøniksen).

http://dx.doi.org/10.1016/j.cemconres.2017.07.012
Received 1 February 2017; Received in revised form 27 July 2017; Accepted 28 July 2017

Table 1
Chemical composition of fly ash (FA) and ground granulated blast furnace slag (GGBFS).

Chemical	FA (wt%)	GGBFS (wt%)
Al_2O_3	25.71	10.65
SiO_2	52.65	34.3
CaO	6.236	43.97
Fe_2O_3	5.307	0.359
MgO	1.402	5.026
K_2O	1.981	0.569
TiO_2	1.2	1.19
Na_2O	1.1	0.28
P_2O_5	1.01	–
SO_3	0.935	3.01
SrO	0.19	–
CO_2	1.74	0.13

MPCM [4,6–8,16]. However, very few studies have examined the mechanical properties of geopolymer compositions with incorporated MPCM [17]. Rasoul et al. [17] observed that the compressive strength of geopolymer mortar decreased after adding PCM, mainly due to the reduced unit weight, and the low strength and stiffness of the PCM. Nevertheless, the compressive strength of geopolymer mortar containing up to 20% PCM was still sufficiently high for applications in buildings.

The main purpose of this study is to examine how incorporation of MPCM influences the mechanical properties of both GPC and PCC at different curing times. Since the state (liquid or solid) of the PCM might influence the compressive strength, the systems have been studied both below and above the melting point of the PCM. The PCM utilized in this study has a melting temperature of about 28 °C, which is suitable for warm climates such as southern Europe [18,19]. In order to gain more information regarding the cause of the reduced compressive strength, we have also investigated how the MPCM alters the microstructures of GPC and PCC.

2. Experimental

2.1. Materials

Geopolymer concrete was prepared by mixing class F fly ash (FA), ground granulated blast furnace slag (GGBFS), sand, gravel, and an alkaline activator solution. The FA (Blaine fineness = 2954 ± 50 cm^2/g, specific gravity = 2.26 ± 0.02 g/cm^3) and GGBFS (Blaine fineness = 3312 ± 50 cm^2/g, specific gravity = 2.85 ± 0.02 g/cm^3) were purchased from Norcem and Cemex, Germany, respectively. Table 1 shows the chemical compositions of class F fly ash and GGBFS which are determined by X-ray Fluorescence (XRF). The alkaline

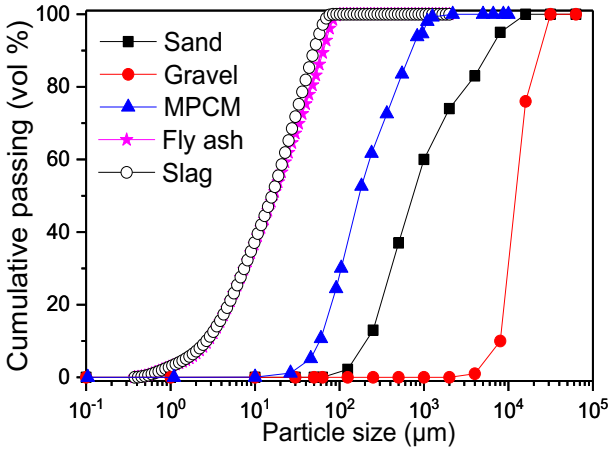

Fig. 2. Particle size distributions of sand, gravel, MPCM, fly ash, and ground granulated blast furnace slag.

solution was prepared by adding sodium hydroxide powder (density 2.1 g/cm^3) to water (14 M), before mixing with sodium silicate solution (50 wt%, density of 1.9 g/cm^3). A sodium silicate solution to sodium hydroxide solution weight ratio of 2.5 was used for all GPC mixtures.

Portland cement concrete consists of Portland cement II mixed with FA (Blaine fineness of 4500 cm^2/g, density of 3.0 g/cm^3), was purchased from Norcem, Norway. Dynamon SR-N (density of 1.1 g/cm^3) from MAPEI, Norway, was used as a superplasticizing admixture to improve the workability of PCC and decrease the amount of water. The same sand (density of 2.7 g/cm^3) and gravel (density of 2.6 g/cm^3) were used for both GPC and PCC, and purchased from Gunnar Holth and Skolt Pukkverk AS, originating from Mysen and Råde, Norway, respectively.

MPCMs (density of 0.9 g/cm^3) was synthesized by spray drying [20]. The MPCM has a copolymer shell consisting of low density polyethylene (LDPE) and ethylvinylacetate (EVA) (EVA/LDPE = 0.5), and contain paraffin wax (Rubitherm®RT27) as the core material (RT27/Polymer = 2). The melting point of MPCMs is 28.4 ± 0.9 °C. The melting point of MPCM should be approximately three degrees higher than the room temperature [18], and near the average temperature of the hottest summer month [19]. The mean particle size of the microcapsules was around 5 μm (Fig. 1a). However, as can be seen from the SEM image in Fig. 1b, the microcapsules have a strong tendency to form agglomerated structures with larger sizes (D60 = 240 μm) [21].

The particle size distribution analysis of sand and gravel was carried out by mechanical sieving according to EN 933-1. The FA and GGBFS

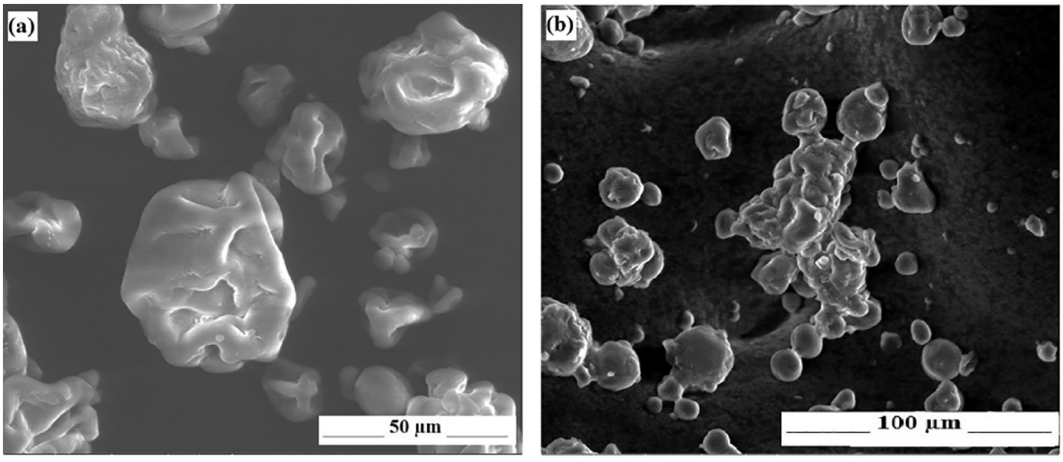

Fig. 1. SEM images of (a) individual MPCM (LDPE.EVA-RT27), (b) agglomeration of MPCM.

Table 2
Mixture design of GPC, amounts represent 1 L of mixture. The MPCM percentages indicate the amount of sand replaced by MPCM.

MPCM (vol%)	Alkaline solution (g)	Water (g)	FA (g)	GGBFS (g)	Sand (g)	Gravel (g)	MPCM (g)
0	161.6	56.4	242.6	161.4	893.1	868.6	0
5	161.6	56.4	242.6	161.4	848.6	868.6	15
10	161.6	56.4	242.6	161.4	803.8	868.6	30
20	161.6	56.4	242.6	161.4	714.5	868.6	60

Table 3
Mixture design of PCC, amounts represent 1 L of mixture. The MPCM percentages indicate the amount of sand replaced by MPCM.

MPCM (vol%)	Cement (g)	Water (g)	Admixture (g)	Sand (g)	Gravel (g)	MPCM (g)
0	434	191.8	5.6	1057	705	0
5	434	192	5.6	1004.2	705	18
10	434	192.2	5.6	951.3	705	36
20	434	192.5	5.6	845.6	705	72

particle size distribution were performed by a laser diffraction particle size analyzer (Beckman-Coulter, LS 13 320 Series). The particle size distribution of MPCM was determined by Low Angle Laser Light Scattering laser diffraction (Malvern Rasterizer 2000). The diameter of the microcapsules was measured to be between 10 and 1000 μm, which confirm the tendency of MPCMs to form agglomerates [21]. Fig. 2 displays the particle size distributions of the utilized materials.

2.2. Mixing methods

In order to prepare GPC and PCC containing PCM, the required amount of PCM in the mixture was determined by its volume percentage and replaced a certain percentage of sand [6]. The percentages given in this paper indicate the amount of sand replaced by MPCM.

2.2.1. GPC mixing method

FA, GGBFS and alkaline solution were mixed together into a homogenous binder. The binder was then introduced into the dried sand and mixed for 30 s. Subsequently, gravel was added to the mixture and mixed for 2 min. Afterwards, the MPCM was added to the mixture and mixing was continued for 2 more minutes.

2.2.2. PCC mixing method

Cement, sand and gravel were mixed together for 2 min. Subsequently, water containing admixture were gradually added and mixed for 1 min. Finally, the MPCM was added to the concrete mixture and mixing was continued for 2 more minutes.

It is noteworthy that for both GPC and PCC, the MPCM was added as the last component in order to limit the damage of the MPCM during the mixing process [6,8]. The summary of mixture designs of GPC and PCC are given in Tables 2 and 3. All components were weighted utilizing a digital balance (BERGMAN) with an accuracy of 0.1 g. The total amount of sand and gravel for the samples without MPCM is approximately the same for GPC and PCC. However, in order to obtain samples with sufficiently high compressive strength while keeping a usable workability of the samples and avoid segregation of the gravel, the ratio between sand and gravel is different for GPC and PCC.

2.2.3. Casting and curing methods

After mixing, GPC and PCC were cast into molds at a size of $10 \times 10 \times 10\ cm^3$. Due to the short setting time of GPC, a vibration machine was used to remove air trapped inside the specimens. The molds were first filled halfway up by fresh GPC and vibrated for 25 s. After this the molds were filled completely and vibrated for further 25 s. For the PCC, half-filled molds were compacted by means of a steel pestle (25 times) and the same procedure was repeated after the molds were filled all the way up. After casting, both GPC and PCC were precured at ambient temperature with a relatively humidity of 90% for 24 h, followed by demolding of the samples. After demolding, the samples were cured in water at either 20 °C (below the melting point of MPCM) or at 40 °C (above the melting point of MPCM) for 1, 3, 7, 14, and 28 days.

2.3. Testing methods

2.3.1. Slump flow test

The workability of fresh GPC and PCC mixtures was measured immediately after mixing by a slump test according to EN 12350-2. An Abrams cone was used as the mold. The cone dimensions were 300 mm in height, and 100 mm and 200 mm in diameters at the top and base, respectively.

2.3.2. Compressive strength test

The compressive strength tests were performed in accordance with EN 12390-3. In this study, the compressive strength was determined using digital compressive strength test machine (Form + Test Machine) with compression capacity of 3000 kN. Each test cube was exposed to a force at a loading rate of 0.8 kN/s until it failed. The compressive strength tests were carried out at 20 °C and 40 °C on GPC and PCC specimens containing 0%, 5%, 10% and 20% MPCM at curing times of 1, 3, 7, 14, and 28 days. For each compression test at 20 °C, three cubes were left in the room for 1 h (to remove free water from the surfaces), before they were weighed and tested. The reported values are the

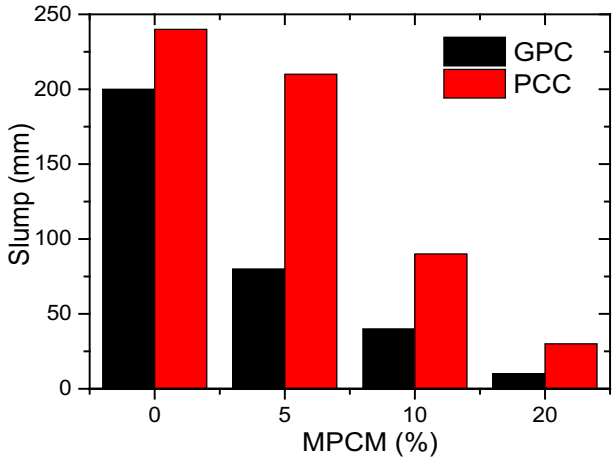

Fig. 3. Slump of GPC and PCC containing various amounts of MPCM.

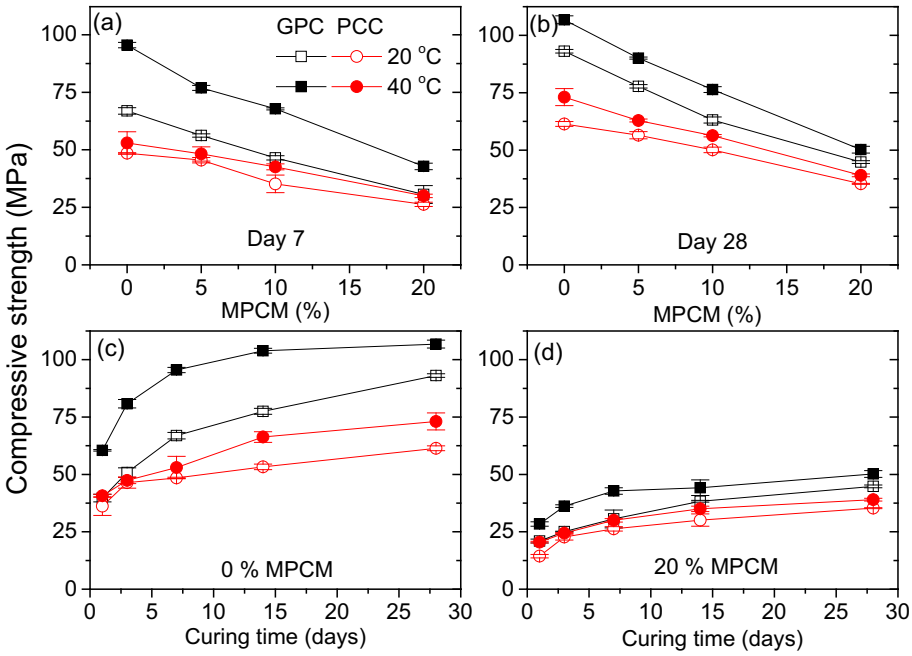

Fig. 4. Compressive strength of GPC and PCC cured at 20 °C and 40 °C (a) versus percentage of sand replaced by MPCM after curing for 7 days (b), curing for 28 days (c) as versus curing time in the absence of MPCM, and (d) versus curing time when 20% of the sand is replaced by MPCM.

average of the three cubes. In order to determine the compressive strength at 40 °C, the compressive strength machine was isolated thermally, and connected to a heating chamber by means of an isolated tube to keep the environmental temperature of the machine constant at 40 °C. Before the compressive strength test, three cubes were kept in a heating chamber at 40 °C for 1 h (to remove free water from the surfaces while keeping the temperature of the cubes constant), immediately afterward the cubes were weighed and tested. The reported values are the average of the three cubes.

2.3.3. X-ray micro-tomography analysis

To study internal microstructure of GPC and PCC, X-ray tomography images from cross-section of specimens in cylindrical form (1 cm diameter and 1 cm height) containing 0 and 20% of MPCM cured at 20 °C were performed using a Skyscan 1172 CT scanner (Bruker) with 85 kV incident radiation, 400 ms exposure time per frame and 0.5° rotation step. The final sets of vertically stacked slices were reconstructed using the Feldkam algorithm [22] and have a voxel size of 10 μm.

Image thresholding based on a minimum cross entropy algorithm [23] was performed in order to convert the slices into binary images. Such images were then used to calculate the equivalent radii (e.g. the radius of a sphere having the same volume as the considered object) of the MPCM present in the samples and their standard deviations of the center-to-surface distance (SD), by using the ImageJ software [24]. The latter parameter is a measure of the deformation of an object (i.e. the extent to which its shape departs from that of a sphere, for which SD = 0).

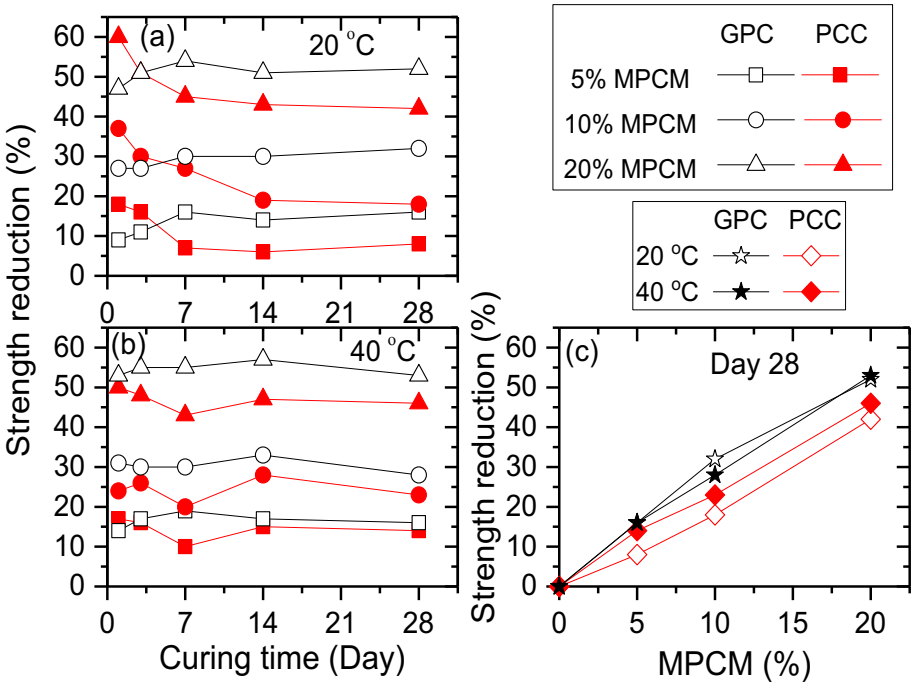

Fig. 5. The compressive strength reduction (percentage compared to samples without MPCM at the same curing time) for GPC and PCC versus curing time at (a) 20 °C and (b) 40 °C, and after 28 days as a function of MPCM concentration (c).

2.3.4. Scanning electron microscopy (SEM) imaging

SEM images from fractured surfaces of GPC and PCC specimens containing 0 and 20% of MPCM cured at 20 and 40 °C were prepared using Quanta FEG-250 Scanning Electron Microscope device at an accelerating voltage of 30 kV. The methods of LFD (Large Field Detector) detector and vCD (Low voltage High Contrast) detector were applied for imaging. The fractured surfaces for SEM images were not polished or coated in order to prevent the effect of coating on the surface.

3. Results and discussion

3.1. Slump flow test

A slump flow test was performed to determine the effect of MPCM addition on the workability of fresh GPC and PCC. The slump test was carried out immediately after mixing GPC or PCC with different amounts of MPCM to obtain the free flow of fresh mixtures. The results are shown in and Fig. 3.

The slump of GPC varied between 10 and 200 mm, whereas PCC showed a slump in the range of 30–230 mm. It is clear from Fig. 3 that increasing the percentage of MPCM from 0 to 20 reduces the workability of both GPC and PCC (markedly lower slump in the presence of MPCM compared to the sample without MPCM). In all cases, the slump of GPC is lower than PCC. This phenomenon has been attributed to the high viscosity of sodium silicate in the alkaline solution making the GPC mixture highly cohesive [25,26]. According to Park et al. [27], the workability of concrete is dependent on the size of the microcapsules. The decrease of the slump flow with the addition of MPCM might therefore be due to differences in the particle size of MPCM compared with the sand it replaces (see Fig. 2).

3.2. Compressive strength

In order to investigate the effect of MPCM on the mechanical properties of the GPC and PCC, the compressive strength was tested at different curing times and temperatures. The results obtained at 20 °C and 40 °C are plotted in. Fig. 4. It should be noted that the samples are both cured and measured at the indicated temperatures, both of which will affect the mechanical properties of the samples.

3.2.1. Effect of MPCM addition

Fig. 4a and b illustrate that the compressive strength of both GPC and PCC decrease with increasing amount of MPCM both at an early age (7 days) and after curing for 28 days at 20 and 40 °C. This decrease might be caused by the lower stiffness and strength of MPCM compared to sand, causing MPCM to be deformed or broken during the compression test [6,17]. PCM might also induce strength reducing voids and air bubbles in concrete [8]. It is also possible that poor bonding and

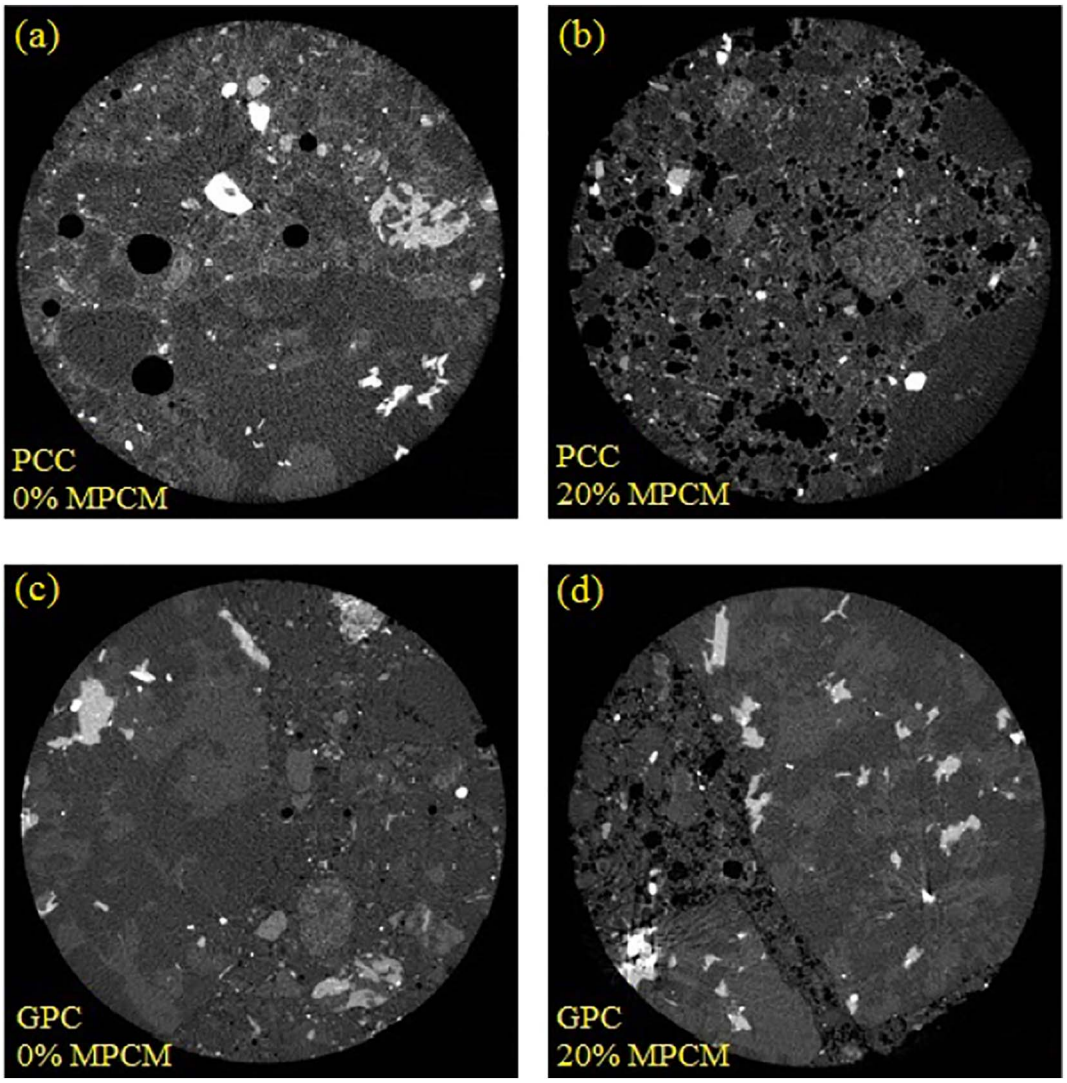

Fig. 6. X-ray-tomography images of samples (a) PCC without MPCM, (b) PCC with 20% MPCM, (c) GPC without MPCM and (d) GPC with 20% MPCM. In these images, dark colors correspond to low or no absorption of X-rays (e.g. air bubbles or microcapsules) and bright colors represent high absorption of X-rays (sand and gravel). The field of view is approximately 1 cm.

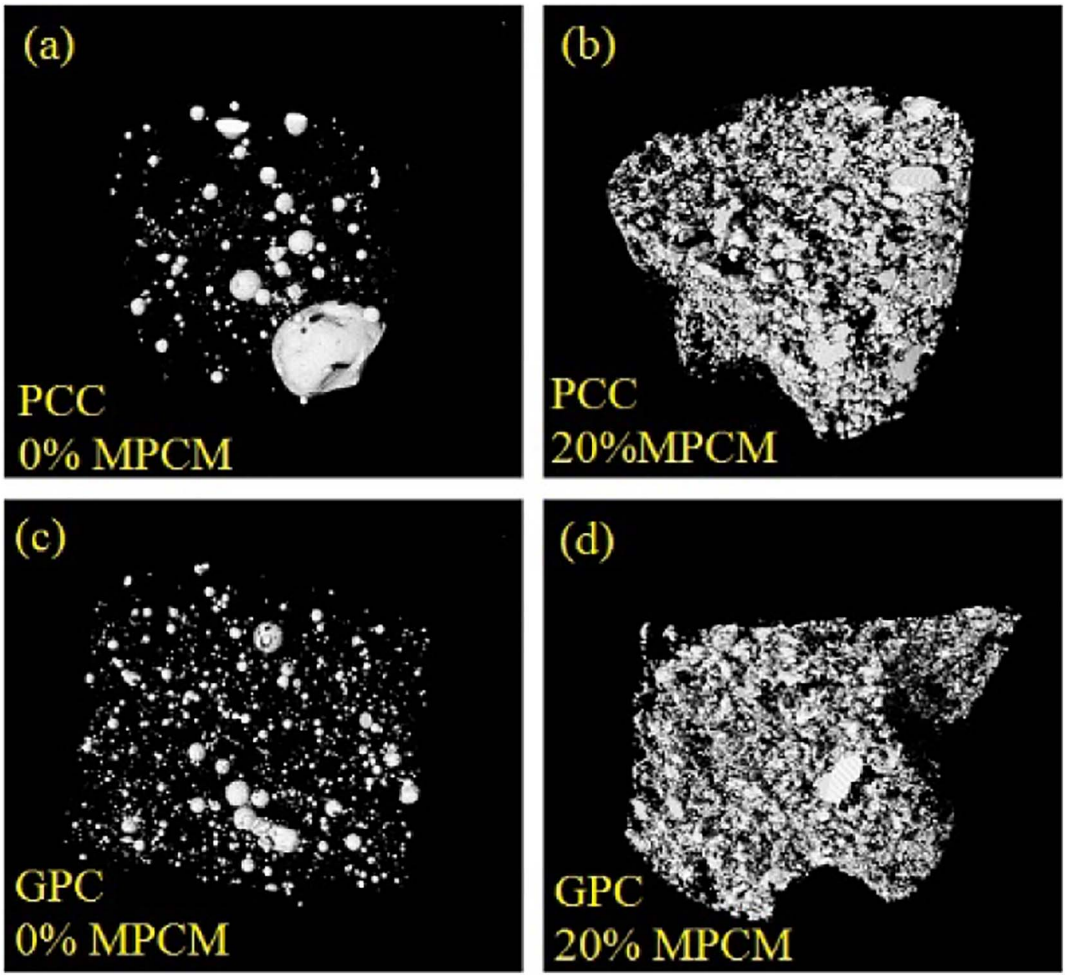

Fig. 7. 3D rendering of air bubbles and MPCM present in cylindrical samples (1 cm diameter) of: (a) PCC without MPCM; (b) PCC with 20% MPCM; (c) GPC without MPCM; (d) GPC with 20% MPCM.

gaps between the MPCM interface and the concrete matrix reduce the compressive strength [9]; these hypotheses will be further discussed in connection with the X-ray tomography and SEM analysis (Sections 3.3 and 3.4) below.

The percentage strength reduction of GPC and PCC compared to samples without MPCM are plotted in Fig. 5. After 28 days, the strength reduction is more pronounced for GPC than for PCC, especially at 20 °C. Low adhesion and weak bonds between MPCM and the concrete matrix may contribute to the strength reduction [9,28].

For GPC cured at 20 °C, the percentage strength reduction increases at short curing times before it stabilizes at a nearly constant value after approximately 1 week. Interestingly, the strength reduction of PCC shows an opposite trend at short curing times. For PCC the strength reduction at 20 °C decreases with curing time, before stabilizing after about 1–2 weeks. The opposite trends at short curing times suggest that the addition of MPCM affects the curing process of GPC and PCC in different ways.

3.2.2. *Effect of curing temperature*

The temperature at which the compressive strength is measured will affect the results. However, the effect of curing temperature can be examined by following the time development of the samples. As can be seen in Fig. 4c and d, curing at a higher temperature accelerates the reaction rates (geopolymerization/hydration). This causes a faster increase of the compressive strength, in agreement with previous findings [14,29–32]. As the compressive strength approaches its final value at long times, the difference between the samples cured at 20 and 40 °C diminishes.

For both GPC and PCC, the effect of curing time on the percentage strength reduction is less obvious at 40 °C than at 20 °C (Fig. 5). This is due to the faster curing at elevated temperatures.

3.2.3. *Effect of solid or liquid PCM*

In order to evaluate the effect of whether the PCM is in solid or liquid state, it is important to minimize the influence of curing conditions on the results. This is facilitated by utilizing the percentage strength reduction compared to a sample without PCM that has experienced the same curing times and temperature (Fig. 5). Since the compressive strength stabilizes at the longest curing times (Fig. 4), the percentage strength reduction at 28 days provides a reasonable estimate of whether the compressive strength of the samples is affected by a solid or liquid state of the PCM. Comparing 20 and 40 °C, there are only small differences in the levels of strength reduction after 28 days for GPC (Fig. 5c). Accordingly, it seems that whether the PCM is in solid or liquid state does not significantly affect the mechanical properties of GPC.

However, unlike GPC, the strength reduction of PCC after 28 days is more pronounced at 40 °C than at 20 °C (Fig. 5c). Accordingly, melting the PCM seems to affect PCC much more than GPC. Melting the PCM can make the microcapsules softer. GPC has a higher compressive strength than PCC, and the stronger matrix might be less affected by the introduction of soft particles. In addition, any PCM that is not properly encapsulated (either from broken capsules or from PCM that is not encapsulated during fabrication) will be in liquid state inside the

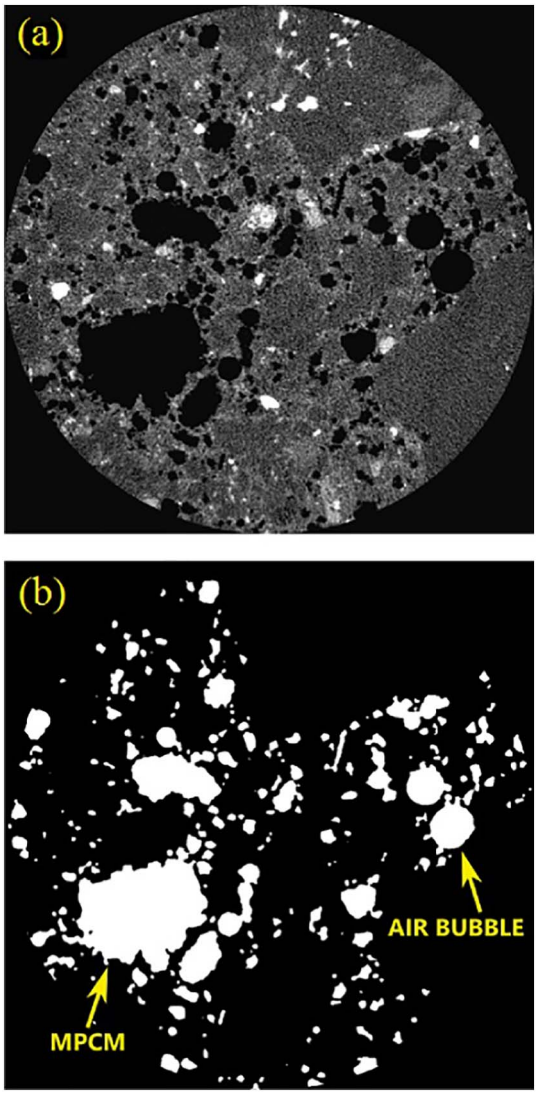

Fig. 8. (a) Grey scale 2D cross sectional slice relative to PCC with 20% MPCM; (b) the same image after conversion to binary. The field of view is approximately 0.9 cm.

concrete matrix. If the MPCM is poorly distributed within the concrete sample, microcapsule agglomerates containing unencapsulated PCM will become much weaker when the PCM is melted. A better distribution with less agglomerated microcapsules in the GPC matrix than in the PCC matrix could explain why the PCC is more affected by melting the PCM. The distribution of microcapsules in the concrete samples will be discussed in connection with the X-ray micro-tomography in Section 3.3 below.

3.3. X-ray micro-tomography

Typical 2D X-ray micro-tomography cross-sectional slices obtained from PCC and GPC, both without and with 20% MPCM, are displayed in Fig. 6. More than 600 2D slices were taken for each sample in order to obtain good statistical data. Fig. 7 displays 3D renderings of the measured samples. The images in Fig. 7 were processed such that only air voids and MPCM are shown.

Given the low level of X-ray attenuation of the organic materials constituting the MPCM, it is not possible to discriminate them from air voids based on grey scale values. However, the discrimination is possible based on shape, which tends to be approximately spherical for air voids, due to interfacial tension effects. The MPCM may have a more irregular shape, as illustrated in Fig. 8.

From a quantitative point of view, the results of the image analysis give a mean value of standard deviation (SD) of 1.36 for PCC in the presence of 20% MPCM compared to a mean value of 0.83 for the plain sample. The mean value of SD increases from 0.56 to 1.24 when 20% MPCM is added to the GPC sample. These values testify to the higher degree of deformation suffered by the MPCM compared to the air bubbles.

A visual inspection of Fig. 7 suggests that a larger number of air voids, having smaller sizes, are present in the GPC sample compared to PCC. This is confirmed by the results of the image analysis, which give a total volume of air voids of approximately 4% for PCC and 6% for GPC. The mean equivalent radius of the air voids drops from 50 μm for PCC to 35 μm for GPC. Such differences might be due to the higher viscosity of the alkaline solution or shorter setting time of fresh GPC, which hinder the coalescence and release of air bubbles. Such a high viscosity, is also testified by slump loss (Fig. 3).

Considering that the unagglomerated single microcapsules have a size of about 50 μm (Fig. 1a), single microcapsules will be difficult to see in the X-ray tomography pictures. Accordingly, the large irregular shapes observed are due to agglomerated microcapsules. From Fig. 6, it can be seen that PCC has agglomerated MPCM distributed throughout the sample, while GPC has some areas with agglomerates and some more homogeneous parts where agglomerates are not observed, which could be due to the gravel. In addition, the agglomerates appear to be larger in the PCC sample. However, it should be noted that the field of view of study is approximately 1 cm, and it may not be representative of the whole concrete sample. As discussed in Section 3.2.3. above, the presence of a high amount of large agglomerates might reduce the compressive strength of PCC when the PCM is melted. The presence of agglomerated structures suggests a poor affinity between the MPCM and the concrete matrix. It is possible that the high viscosity (low workability) of the pre-set GPC and the short setting times of GPC help prevent the formation of MPCM agglomerates.

3.4. SEM analysis

The PCC and GPC samples with 20% MPCM after 28 days curing at 20 and 40 °C were chosen for SEM analysis. Images in Fig. 9a, b, c and d are taken by vCD (Z compositional detector) to illustrate the organic (MPCM) and inorganic (concrete matrix) components. In these images, the organic MPCM will appear as darker areas in contrast to the brighter concrete matrix. Images of the same areas (Fig. 9A, B, C, D), taken with LFD (Morphological detector) show the topography of the sample (bright areas are extending higher up than dark areas). Accordingly, areas that are dark in vCD and light in LFD are microcapsules. Comparing vCD and LFD it is obvious that there are gaps between the MPCM particles and the concrete matrix. Similar observations have been reported previously [7,21].

The gaps between the microcapsules and the concrete indicate that the connection between the MPCM and the surrounding matrix is weak, and that MPCM may induce air voids in the samples. There are several mechanisms that might cause these gaps. The tendency of MPCM to agglomerate into larger structures reduces the ability of the MPCM to fill in the cavities in the concrete structure [7,33-35], thereby inducing air voids. In addition, a poor compatibility between the microcapsules and the concrete matrix can cause voids to be formed between them. A poor compatibility indicates that the shell of the microcapsules does not bond nor associate with the concrete matrix. Other kinds of microcapsules did not exhibit this problem [16], which illustrates the importance of a good compatibility between the shell of the microcapsules and the concrete matrix. Accordingly, the shell used in the current MPCM is probably not optimal for inclusion in concrete structures.

The air voids are probably an important contributing factor to the compressive strength reduction in the presence of MPCM. Accordingly, the SEM results can help to explain the reduced compressive strength induced by the addition of MPCM to PCC and GPC, as described in Section 3.2 above.

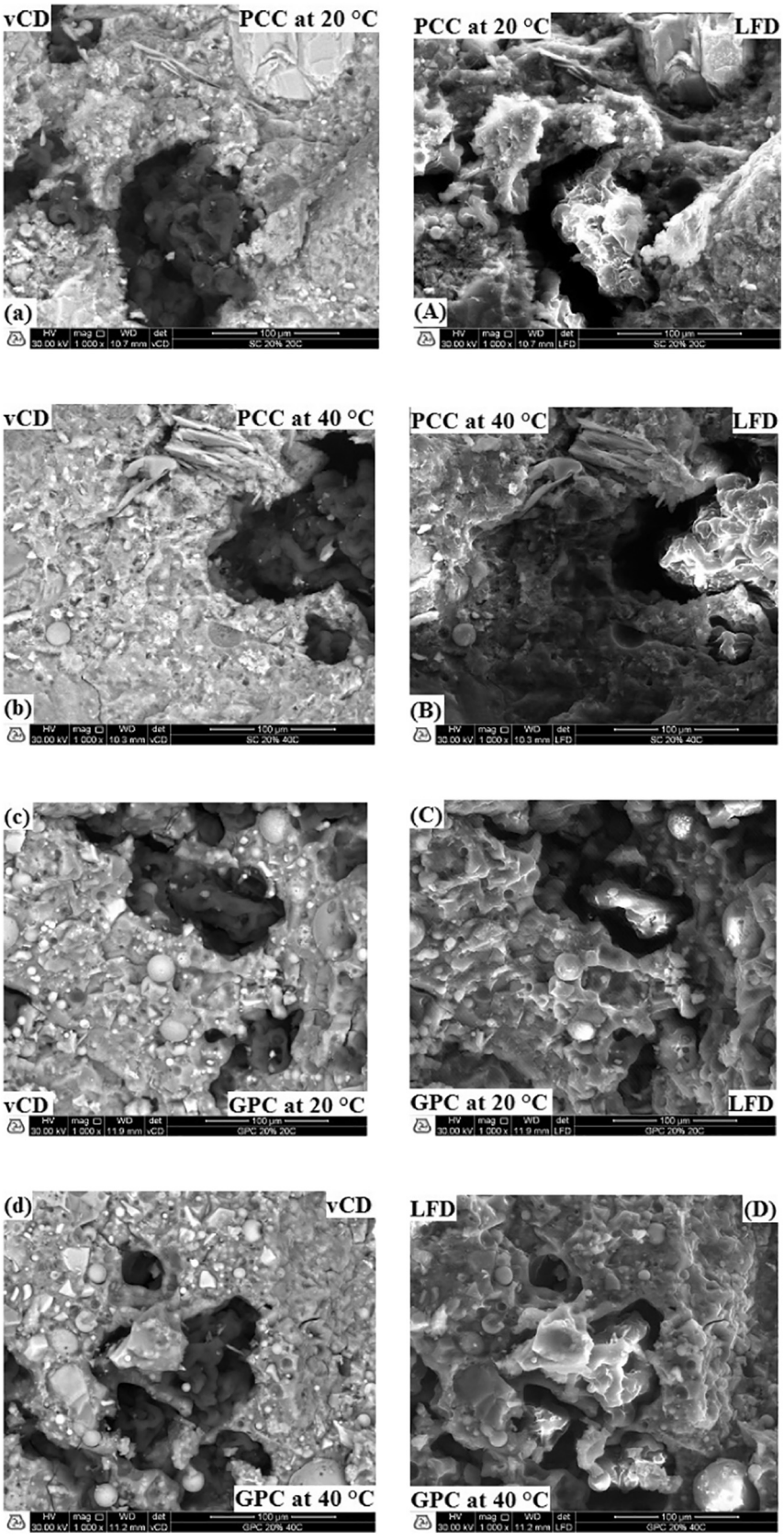

Fig. 9. SEM images of fracture surface of 20% MPCM incorporated in (a) PCC at 20 °C, (b) PCC at 40 °C, (c) GPC at 20 °C, and (d) GPC at 40 °C (by vCD detector), (A) PCC at 20 °C, (B) PCC at 40 °C, (C) GPC at 20 °C, and (D) GPC at 40 °C (by LFD detector). MPCM will show up as dark areas in vCD and bright areas in LDF, while voids will be dark in both types of images.

4. Conclusions

In this study, the effect of MPCM in solid and liquid states on the physical and mechanical properties of GPC and PCC was investigated.

It was found that increasing the percentage of MPCM from 0 to 20 reduced the workability of both GPC and PCC. In all cases, the slump of GPC was lower than PCC due to the high viscosity of the alkaline solution. The compressive strength of both GPC and PCC decreased with increasing amount of MPCM at both 20 and 40 °C. SEM images reveal weak connections and air voids between the MPCM and the surrounding matrix, which will contribute to the strength reduction of concrete with incorporated MPCM.

Whether the PCM is in solid or liquid state does not significantly affect the mechanical properties of GPC. However, the addition of MPCM to PCC induced a compressive strength reduction, which seemed to be affected by the state (solid or liquid) of the PCM. These results could indicate that GPC is a more suitable option for concrete with incorporated MPCM, when these building materials are exposed to changes in temperature. However, despite the negative effect of the MPCMs on the compressive strength of GPC and PCC, the compressive strength is still sufficiently high for structural applications (acceptable range of compressive strength is between 25 and 40 MPa).

Acknowledgement

This work was supported by The Research Council of Norway, grant number 238198. We would like to thank Trond Atle Drøbak and Inge Richard Eeg for technical assistance.

References

[1] T.-C. Ling, C.-S. Poon, Use of phase change materials for thermal energy storage in concrete: an overview, Constr. Build. Mater. 46 (2013) 55–62.
[2] A.F. Regin, S.C. Solanki, J.S. Saini, Heat transfer characteristics of thermal energy storage system using PCM capsules: a review, Renew. Sust. Energ. Rev. 12 (2008) 2438–2458.
[3] A. Pasupathy, R. Velraj, R.V. Seeniraj, Phase change material-based building architecture for thermal management in residential and commercial establishments, Renew. Sust. Energ. Rev. 12 (2008) 39–64.
[4] C. Norvell, D.J. Sailor, P. Dusicka, The effect of microencapsulated phase-change material on the compressive strength of structural concrete, J. Green Build. 8 (2013) 116–124.
[5] A. Figueiredo, J. Lapa, R. Vicente, C. Cardoso, Mechanical and thermal characterization of concrete with incorporation of microencapsulated PCM for applications in thermally activated slabs, Constr. Build. Mater. 112 (2016) 639–647.
[6] M. Pania, X. Yunping, Effect of phase-change materials on properties of concrete, ACI Mater. J. 109 (2012) 71–80.
[7] M. Hunger, A.G. Entrop, I. Mandilaras, H.J.H. Brouwers, M. Founti, The behavior of self-compacting concrete containing micro-encapsulated phase change materials, Cem. Concr. Compos. 31 (2009) 731–743.
[8] T. Lecompte, P. Le Bideau, P. Glouannec, D. Nortershauser, S. Le Masson, Mechanical and thermo-physical behaviour of concretes and mortars containing phase change material, Energy Build. 94 (2015) 52–60.
[9] H. Cui, W. Liao, X. Mi, T.Y. Lo, D. Chen, Study on functional and mechanical properties of cement mortar with graphite-modified microencapsulated phase-change materials, Energy and Buildings 105 (2015) 273–284.
[10] B. Singh, G. Ishwarya, M. Gupta, S.K. Bhattacharyya, Geopolymer concrete: a review of some recent developments, Constr. Build. Mater. 85 (2015) 78–90.
[11] P. Duxson, J.L. Provis, G.C. Lukey, J.S.J. van Deventer, The role of inorganic polymer technology in the development of 'green concrete', Cem. Concr. Res. 37 (2007) 1590–1597.
[12] L.N. Assi, E. Deaver, M.K. ElBatanouny, P. Ziehl, Investigation of early compressive strength of fly ash-based geopolymer concrete, Constr. Build. Mater. 112 (2016) 807–815.
[13] K.T. Nguyen, N. Ahn, T.A. Le, K. Lee, Theoretical and experimental study on mechanical properties and flexural strength of fly ash-geopolymer concrete, Constr. Build. Mater. 106 (2016) 65–77.
[14] G.S. Ryu, Y.B. Lee, K.T. Koh, Y.S. Chung, The mechanical properties of fly ash-based geopolymer concrete with alkaline activators, Constr. Build. Mater. 47 (2013) 409–418.
[15] J. Temuujin, A. van Riessen, K.J.D. MacKenzie, Preparation and characterisation of fly ash based geopolymer mortars, Constr. Build. Mater. 24 (2010) 1906–1910.
[16] M. Aguayo, S. Das, A. Maroli, N. Kabay, J.C.E. Mertens, S.D. Rajan, G. Sant, N. Chawla, N. Neithalath, The influence of microencapsulated phase change material (PCM) characteristics on the microstructure and strength of cementitious composites: experiments and finite element simulations, Cem. Concr. Compos. 73 (2016) 29–41.
[17] R. Shadnia, L. Zhang, P. Li, Experimental study of geopolymer mortar with incorporated PCM, Constr. Build. Mater. 84 (2015) 95–102.
[18] K. Peippo, P. Kauranen, P.D. Lund, A multicomponent PCM wall optimized for passive solar heating, Energy and Buildings 17 (1991) 259–270.
[19] S. Medved, C. Arkar, Correlation between the local climate and the free-cooling potential of latent heat storage, Energy and Buildings 40 (2008) 429–437.
[20] A.M. Borreguero, J.L. Valverde, J.F. Rodríguez, A.H. Barber, J.J. Cubillo, M. Carmona, Synthesis and characterization of microcapsules containing Rubitherm®RT27 obtained by spray drying, Chem. Eng. J. 166 (2011) 384–390.
[21] V.D. Cao, S. Pilehvar, C. Salas-Bringas, A.M. Szczotok, J.F. Rodriguez, M. Carmona, N. Al-Manasir, A.-L. Kjøniksen, Microencapsulated phase change materials for enhancing the thermal performance of Portland cement concrete and geopolymer concrete for passive building applications, Energy Convers. Manag. 133 (2017) 56–66.
[22] L. Feldkamp, L. Davis, J. Kress, Practical cone-beam algorithm, J. Opt. Soc. Am. A 1 (1984) 612–619.
[23] C. Li, P.K.-S. Tam, An iterative algorithm for minimum cross entropy thresholding, Pattern Recogn. Lett. 19 (1998) 771–776.
[24] C.A. Schneider, W.S. Rasband, K.W. Eliceiri, NIH image to ImageJ: 25 years of image analysis, Nat. Methods 9 (2012) 671–675.
[25] P.S. Deb, P. Nath, P.K. Sarker, The effects of ground granulated blast-furnace slag blending with fly ash and activator content on the workability and strength properties of geopolymer concrete cured at ambient temperature, Mater. Des. 62 (2014) 32–39.
[26] P. Nath, P.K. Sarker, Effect of GGBFS on setting, workability and early strength properties of fly ash geopolymer concrete cured in ambient condition, Constr. Build. Mater. 66 (2014) 163–171.
[27] S.-K. Park, J.-H.J. Kim, J.-W. Nam, H.D. Phan, J.-K. Kim, Development of antifungal mortar and concrete using zeolite and zeocarbon microcapsules, Cem. Concr. Compos. 31 (2009) 447–453.
[28] S. Cunha, J. Aguiar, F. Pacheco-Torgal, Effect of temperature on mortars with incorporation of phase change materials, Constr. Build. Mater. 98 (2015) 89–101.
[29] P. Rovnaník, Effect of curing temperature on the development of hard structure of metakaolin-based geopolymer, Constr. Build. Mater. 24 (2010) 1176–1183.
[30] A.F. Bingöl, İ. Tohumcu, Effects of different curing regimes on the compressive strength properties of self-compacting concrete incorporating fly ash and silica fume, Mater. Des. 51 (2013) 12–18.
[31] A. Allahverdi, S. Pilehvar, M. Mahinroosta, Influence of curing conditions on the mechanical and physical properties of chemically-activated phosphorous slag cement, Powder Technol. 288 (2016) 132–139.
[32] D. Khale, R. Chaudhary, Mechanism of geopolymerization and factors influencing its development: a review, J. Mater. Sci. 42 (2007) 729–746.
[33] P.K. Dehdezi, M.R. Hall, A.R. Dawson, S.P. Casey, Thermal, mechanical and microstructural analysis of concrete containing microencapsulated phase change materials, Int. J. Pavement Eng. 14 (2013) 449–462.
[34] A.M. Borreguero, A. Serrano, I. Garrido, J.F. Rodríguez, M. Carmona, Polymeric-SiO2-PCMs for improving the thermal properties of gypsum applied in energy efficient buildings, Energy Convers. Manag. 87 (2014) 138–144.
[35] H. Moosberg-Bustnes, B. Lagerblad, E. Forssberg, The function of fillers in concrete, Mater. Struct. 37 (2004) 74–81.